

Dynamic Distribution of SeqA Protein across the Chromosome of *Escherichia coli* K-12

María Antonia Sánchez-Romero,^a Stephen J. W. Busby,^a Nigel P. Dyer,^b Sascha Ott,^b Andrew D. Millard,^c and David C. Grainger^c

School of Biosciences, the University of Birmingham, Edgbaston, Birmingham, United Kingdom^a; Systems Biology Centre, Coventry House, the University of Warwick, Coventry, United Kingdom^b; and Department of Biological Sciences, the University of Warwick, Coventry, United Kingdom^c

ABSTRACT The bacterial SeqA protein binds to hemi-methylated GATC sequences that arise in newly synthesized DNA upon passage of the replication machinery. In *Escherichia coli* K-12, the single replication origin *oriC* is a well-characterized target for SeqA, which binds to multiple hemi-methylated GATC sequences immediately after replication has initiated. This sequesters *oriC*, thereby preventing reinitiation of replication. However, the genome-wide DNA binding properties of SeqA are unknown, and hence, here, we describe a study of the binding of SeqA across the entire *Escherichia coli* K-12 chromosome, using chromatin immunoprecipitation in combination with DNA microarrays. Our data show that SeqA binding correlates with the frequency and spacing of GATC sequences across the entire genome. Less SeqA is found in highly transcribed regions, as well as in the *ter* macrodomain. Using synchronized cultures, we show that SeqA distribution differs with the cell cycle. SeqA remains bound to some targets after replication has ceased, and these targets locate to genes encoding factors involved in nucleotide metabolism, chromosome replication, and methyl transfer.

IMPORTANCE DNA replication in bacteria is a highly regulated process. In many bacteria, a protein called SeqA plays a key role by binding to newly replicated DNA. Thus, at the origin of DNA replication, SeqA binding blocks premature reinitiation of replication rounds. Although most investigators have focused on the role of SeqA at replication origins, it has long been suspected that SeqA has a more pervasive role. In this study, we describe how we have been able to identify scores of targets, across the entire *Escherichia coli* chromosome, to which SeqA binds. Using synchronously growing cells, we show that the distribution of SeqA between these targets alters as replication of the chromosome progresses. This suggests that sequential changes in SeqA distribution orchestrate a program of gene expression that ensures coordinated DNA replication and cell division.

Received 4 February 2010 Accepted 10 February 2010 Published 18 May 2010

Citation Sánchez-Romero, M. A., S. J. W. Busby, N. P. Dyer, S. Ott, A. D. Millard, and D. C. Grainger. 2010. Dynamic distribution of SeqA protein across the chromosome of *Escherichia coli* K-12. *mBio* 1(1):e00012-10. doi:10.1128/mBio.00012-10.

Editor Sang Yup Lee, Korea Advanced Institute of Science and Technology

Copyright © 2010 Sánchez-Romero et al. This is an open-access article distributed under the terms of the Creative Commons Attribution-Noncommercial-Share Alike 3.0 Unported License, which permits unrestricted noncommercial use, distribution, and reproduction in any medium, provided the original author and source are credited.

Address correspondence to David C. Grainger, d.c.grainger@warwick.ac.uk.

In the bacterium *Escherichia coli*, chromosome replication initiates bidirectionally from a single locus, *oriC*, and terminates at the diametrically opposed *ter* region (1). Chromosome replication is triggered by the binding of the DnaA initiator protein to multiple sites at *oriC*, and this promotes unwinding of adjacent AT-rich DNA tracts (2–4). Once the DNA duplex has been opened, DnaC facilitates loading of the DnaB helicase and the replication apparatus can initiate chromosome replication (5). Chromosome replication has to be coordinated with the cell cycle to ensure that each replication origin fires only once and that progeny receive the correct number of chromosomes (6). New copies of *oriC* must be silenced to prevent secondary initiation events from occurring, and DNA methylation patterns are exploited to identify newly made *oriC*. Briefly, the *oriC* region is enriched with GATC motifs, which are targets for the Dam methylase that methylates the adenine in GATC sequences (7). At each target, both strands of the DNA double helix can be methylated, but because there is a lag between DNA synthesis and methylation, new copies of *oriC* are transiently hemi-methylated (i.e., methylated on only the template DNA strand). These transients are recognized by SeqA protein, which preferentially binds as a dimer to pairs of hemi-

methylated GATC sites (8, 9). This binding sequesters *oriC*, thereby retarding full methylation and the binding of DnaA (10–12). This is believed to be a key regulatory mechanism in the control of bacterial chromosome replication.

There are 19,120 GATC motifs scattered throughout the *E. coli* K-12 chromosome, and these sites may also serve as binding targets for SeqA. Probably the best-known example is the *dnaA* gene and *dnaAp₂* promoter, which are located close to *oriC* and contain multiple GATC sites. When hemi-methylated, SeqA is able to bind to these sites and repress *dnaA* transcription 10-fold, presumably by occluding binding of RNA polymerase. Repression is transient and is relieved when the region becomes fully methylated by Dam, which competes with SeqA for binding at GATC motifs (13, 14). Thus, SeqA can regulate the initiation of replication by modulating DnaA levels as well as by sequestering *oriC*. Regulation by SeqA has also been shown at bacteriophage λ promoters and the *Salmonella enterica* *std* fimbrial operon, indicating that *dnaA* is not an isolated example of specific gene regulation by SeqA (15, 16).

The extent of the SeqA regulon in *E. coli* remains an open question. The DNA binding properties of SeqA have been meticulously studied at particular loci using *in vitro* DNA binding assays

(8, 9, 17–20) and indirect *in vivo* methods (13, 14) but not on a genome-wide scale. Thus, Løbner-Olesen and colleagues (21) used transcriptomic approaches to investigate the *E. coli* SeqA regulon, but they found few connections between genes affected in a *seqA* mutant and the occurrence of GATC motifs, suggesting that many of the observed effects were indirect. Here, we have exploited chromatin immunoprecipitation (ChIP) to study the genome-wide distribution of SeqA protein. Recall that ChIP is a technique that permits the direct measurement *in vivo* of the binding of any factor to specific chromosome locations and that it can be applied easily to measure factor binding across whole chromosomes (22, 23). For *E. coli*, ChIP applications so far have focused mainly on RNA polymerase, transcription factors, and chromosome folding proteins (24), but proteins involved in DNA replication and its regulation have been studied in *Bacillus subtilis* (25, 26). In the present study, we have used ChIP in combination with microarrays (ChIP-chip) to compare SeqA binding patterns in unsynchronized, synchronized, and nonreplicating cultures of *E. coli*. We pinpoint the most stable SeqA binding loci and report that some of these coincide with genes encoding key proteins involved in cell division. We have also compared patterns of SeqA and RNA polymerase binding to show that there is an inverse correlation between transcription and SeqA binding.

RESULTS

Experimental design and generation of ChIP-chip data. Our aim was to exploit ChIP-chip to determine the chromosome-wide DNA binding properties of SeqA. Since SeqA binding is dependent on the methylation state of the DNA, and thus the position of cells within the cell cycle, we have worked with *E. coli* K-12 strain CMT940, which carries the *dnaC2* temperature-sensitive allele (27). CMT940 cells grow normally at 30°C. However, upon shift to 42°C, they are unable to initiate new rounds of DNA replication, but importantly, rounds of replication that are already under way are completed. Cells can then be returned to 30°C to initiate synchronous chromosome replication. We selected 42°C for the nonpermissive temperature since it provides the most stringent inhibition of new replication rounds without affecting the kinetics of replication runout (28). Figure 1A shows a trace of [³H]thymidine incorporation in a CMT940 culture subjected to these temperature shifts. The data confirm that thymidine incorporation rates fall rapidly after cells are transferred from 30°C to 42°C and that, after 60 min, DNA replication has ceased. Thymidine incorporation increased 6-fold within minutes of cells being returned to 30°C. Complementary flow cytometry experiments presented in Fig. 1B show the number of chromosome equivalents for CMT940 cells at each temperature. Thus, CMT940 cells in unsynchronized cultures contain ~1.5 chromosomes; this decreases to 1.0 chromosome per cell after 60 min at 42°C, and when cultures are returned to 30°C, the number of chromosomes increases. Crucially, after 60 min at 42°C, >90% of the replication rounds had run to completion.

For the ChIP-chip experiments described here, we harvested cells at three time points (Fig. 1A). Thus, for each ChIP-chip replicate, three cultures of CMT940 were grown at 30°C for 1 h and were thus unsynchronized. At this point (time point A), one of the cultures was harvested for ChIP-chip analysis and the two remaining cultures were shifted to 42°C. After an hour, at which point replication events were complete (29), a second culture was harvested for analysis (time point B). The remaining culture was then

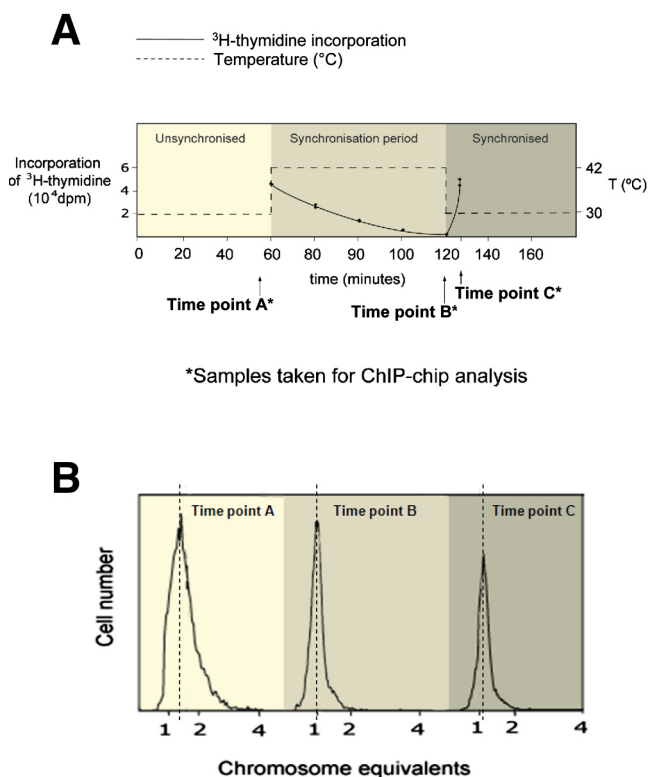


FIG 1 Time course of temperature shifts used to generate *E. coli* cultures for ChIP-chip analysis. The *E. coli* strain CMT940 used for these experiments carries the *dnaC2* allele and can initiate chromosome replication normally at 30°C but not at 42°C. (A) Rates of DNA synthesis measured by thymidine incorporation (solid line) at different temperatures (dotted line) and the time points (A, B, and C) at which cultures were harvested for analysis. (B) Results from flow cytometry experiments with CMT940 cells at each time point.

returned to 30°C, allowing synchronous initiation of chromosome replication, and harvested after 6 min (time point C). For each ChIP-chip experiment, DNA immunoprecipitated with anti-SeqA was labeled with Cy5 and DNA from a mock immunoprecipitation with no antibody was labeled with Cy3. Thus, DNA microarray probes with an elevated Cy5/Cy3 ratio correspond to regions of the genome bound by SeqA.

Overview of chromosome-wide SeqA binding. Figure 2 shows an overview of the SeqA binding profile at time points A, B, and C, derived from ChIP-chip data and plotted against the basic features of the *E. coli* chromosome and the local density of GATC motifs. In unsynchronized cells, the largest SeqA binding signal corresponds exactly with the location of *oriC* (Fig. 2A). A clear signal for SeqA binding is observed at the nearby *dnaA* locus, with binding being spread across the entire gene (see Fig. S1 in the supplemental material). Further SeqA binding signals, comparable in intensity to the signal seen at *dnaA*, are scattered throughout the genome, and these correspond well to locations where the frequency of GATC sites is higher (some examples are shown in Fig. S2 in the supplemental material). One hundred thirty-seven genes have a SeqA binding signal >4-fold above background levels (see Table S7 in the supplemental material). Of these genes, 24 are directly involved in nucleotide metabolism, DNA repair/replication, or methyl group transfer. Interestingly, SeqA binding across an ~1.3-Mbp segment that includes the *ter* region is greatly

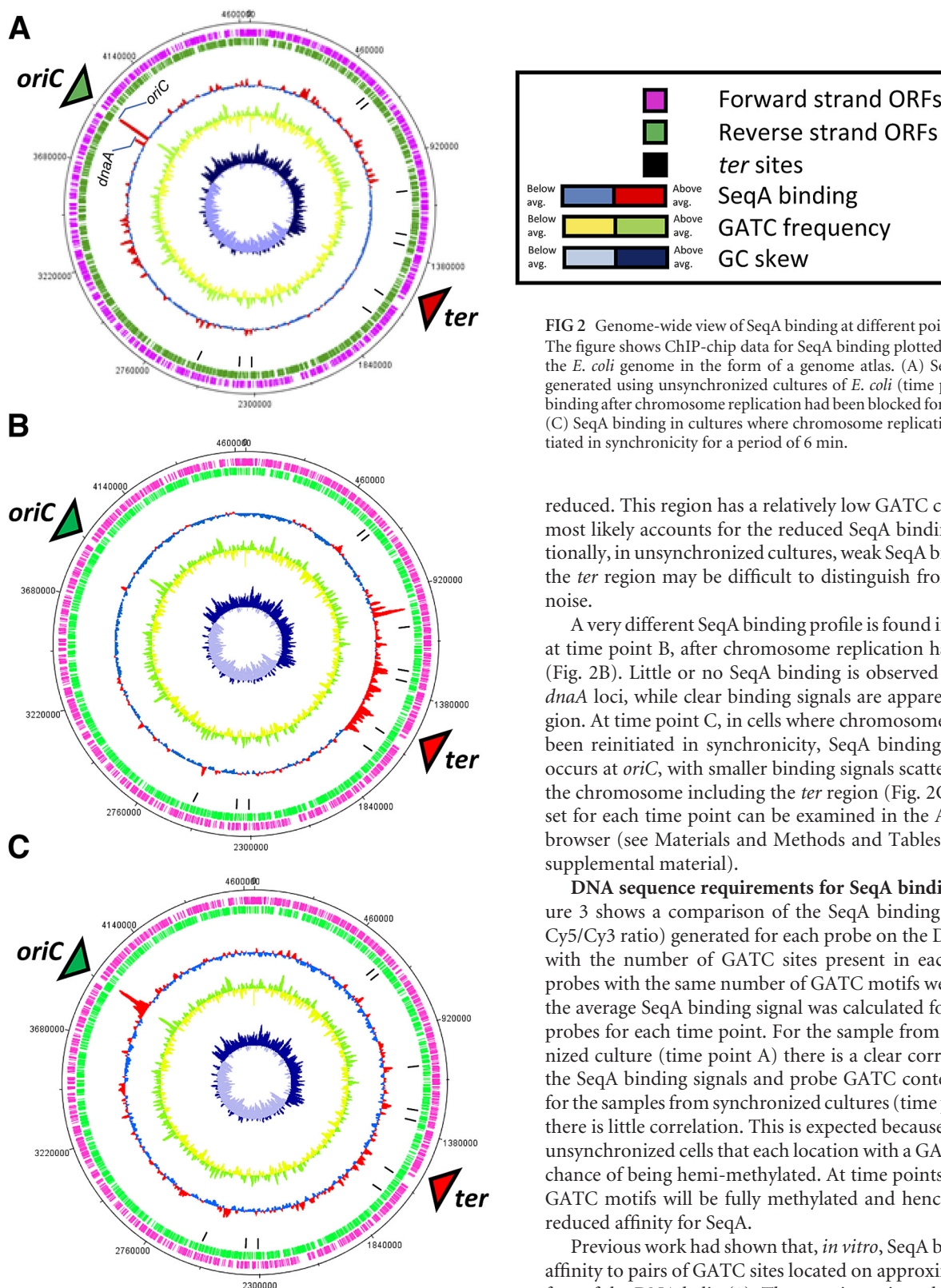


FIG 2 Genome-wide view of SeqA binding at different points in the cell cycle. The figure shows ChIP-chip data for SeqA binding plotted against features of the *E. coli* genome in the form of a genome atlas. (A) SeqA binding signal generated using unsynchronized cultures of *E. coli* (time point A); (B) SeqA binding after chromosome replication had been blocked for 1 h (time point B); (C) SeqA binding in cultures where chromosome replication had been reinitiated in synchronicity for a period of 6 min.

reduced. This region has a relatively low GATC content, and this most likely accounts for the reduced SeqA binding signal. Additionally, in unsynchronized cultures, weak SeqA binding signals in the *ter* region may be difficult to distinguish from experimental noise.

A very different SeqA binding profile is found in cells harvested at time point B, after chromosome replication has been blocked (Fig. 2B). Little or no SeqA binding is observed at the *oriC* and *dnaA* loci, while clear binding signals are apparent in the *ter* region. At time point C, in cells where chromosome replication has been reinitiated in synchronicity, SeqA binding predominantly occurs at *oriC*, with smaller binding signals scattered throughout the chromosome including the *ter* region (Fig. 2C). The full data set for each time point can be examined in the Artemis genome browser (see Materials and Methods and Tables S1 to S6 in the supplemental material).

DNA sequence requirements for SeqA binding in vivo. Figure 3 shows a comparison of the SeqA binding signal (i.e., the Cy5/Cy3 ratio) generated for each probe on the DNA microarray with the number of GATC sites present in each probe. Thus, probes with the same number of GATC motifs were grouped and the average SeqA binding signal was calculated for each group of probes for each time point. For the sample from the unsynchronized culture (time point A) there is a clear correlation between the SeqA binding signals and probe GATC content. In contrast, for the samples from synchronized cultures (time points B and C), there is little correlation. This is expected because it is only in the unsynchronized cells that each location with a GATC has an equal chance of being hemi-methylated. At time points B and C, many GATC motifs will be fully methylated and hence have a greatly reduced affinity for SeqA.

Previous work had shown that, *in vitro*, SeqA binds with a high affinity to pairs of GATC sites located on approximately the same face of the DNA helix (8). Thus, we investigated the relationship between adjacent GATC motif spacing and the SeqA binding signal at time point A. Regions of the genome with a SeqA binding signal greater than 1.5 were selected, and the spacing between adjacent GATC motifs was determined for these regions. As a

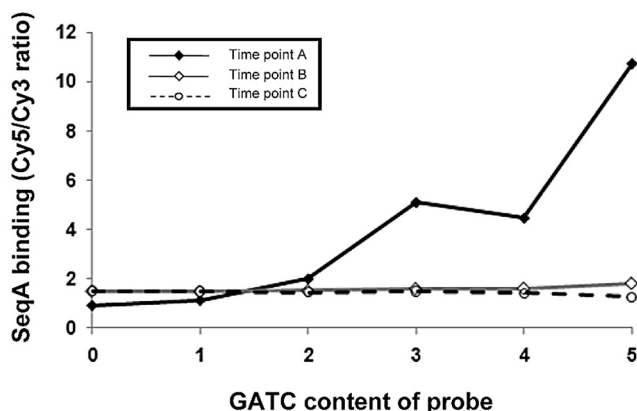


FIG 3 Relationship between SeqA binding and the occurrence of GATC motifs *in vivo*. The SeqA binding values are Cy5/Cy3 ratios generated from ChIP experiments analyzed using a DNA microarray. DNA microarray probes were grouped according to the number of GATC motifs present in the probe, and the average Cy5/Cy3 ratio was calculated for each group of probes. Data presented were generated from unsynchronized cultures of *E. coli* (time point A), cultures where chromosome replication had been blocked for 1 h (time point B), and cultures where chromosome replication had been reinitiated in synchronicity for a period of 6 min (time point C).

control, we also determined the spacing between GATC motifs for the entire *E. coli* genome. The results of this analysis are plotted as a histogram in Fig. 4. For regions of the genome bound by SeqA, adjacent GATC sites are most frequently separated by close to 10 or 20 bp and there is a clear preference for adjacent GATC motifs to be located closer than ~50 bp apart (Fig. 4A). When the entire genome was analyzed in the same way, a different pattern of GATC motif spacing was observed (Fig. 4B). Note that when the entire genome is considered, periodicity can be observed in the frequency of GATC motif spacing. This is likely a consequence of codon usage.

Identification of stable SeqA binding targets. The ChIP-chip analysis of SeqA binding identifies many previously unknown SeqA binding loci. To identify the targets where SeqA association is the most stable, we selected regions that gave a strong SeqA binding signal in both unsynchronized cultures (time point A) and cultures where DNA replication had ceased (time point B). Our reasoning was that the experiment with the unsynchronized culture would identify a large number of targets, while the locations bound by SeqA after chromosome replication was blocked must retain SeqA for longer times. The 12 top targets are listed in Table 1. Strikingly, six of these have roles in DNA synthesis, chromosome replication, or methyl group transfer, and all are located at regions with an above-average density of GATC motifs. Figure 5A shows data for the *pyrD-rlmL-uup* locus, where the *pyrD* gene encodes an enzyme involved in pyrimidine nucleotide synthesis, *rlmL* encodes a methyltransferase, and *uup* encodes a protein involved in replication fork progression. All three genes are covered by SeqA, and binding coincides with a high density of GATC motifs. Figure 5B shows similar results with the *mukFEB* operon, which encodes proteins involved in chromosome segregation, and the adjacent *smtA* gene, which encodes a methyltransferase. Note that binding of SeqA close to both the *pyrD* and *mukF* regions is greatly reduced at time point C, shortly after the initiation of a replication round, presumably because SeqA is titrated

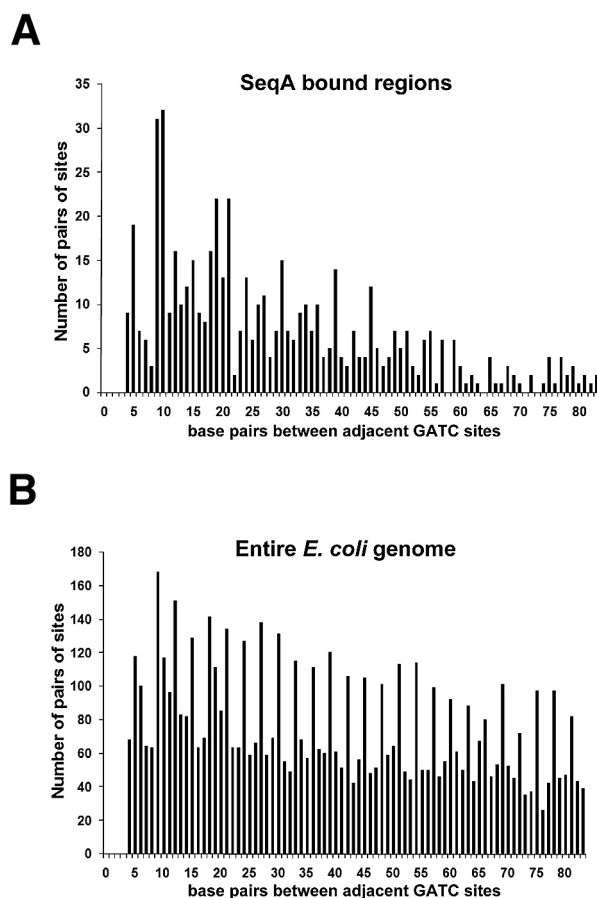


FIG 4 Spacing of adjacent GATC motifs across the whole *E. coli* genome and in genomic regions bound by SeqA. The spacings between adjacent GATC motifs across regions of the *E. coli* genome bound by SeqA at time point A (A) and the entire *E. coli* genome (B) were compared. The data show that, *in vivo*, a gap of close to 10 or 20 nucleotides between GATC motifs is most favorable for SeqA binding.

off these targets due to increased hemi-methylation of DNA close to *oriC*.

Relationship between SeqA and RNA polymerase binding. Our initial attempts to detect effects of SeqA on transcription, using reverse transcription (RT)-PCR and RNA extracted from CMT940 cells at different time points, was uninformative (data not shown). For example, we saw no changes in *mukF* and *pyrD* mRNA levels between time points B and C, despite SeqA binding at these loci and altering substantially (Fig. 5). We reasoned that a better strategy would be to compare genome-wide patterns of SeqA and RNA polymerase binding in unsynchronized cultures (time point A) using ChIP-chip (30). Thus, problems due to low levels of many transcripts, RNA instability, and cell cycle-dependent effects on gene transcription were avoided. Our data show that regions with a strong SeqA binding signal (for example, the locations listed in Table 1) tend to give a low RNA polymerase binding signal, while locations with a strong RNA polymerase binding signal (for example, the rRNA operons) are not bound by SeqA. Some examples of binding profiles are shown in Fig. S4 in the supplemental material, which shows an overall negative correlation between the binding of SeqA and RNA polymerase. The

TABLE 1 Stable SeqA targets outside the replication origin

Gene	Function(s)	SeqA binding signal ^a	Length (bp)	No. of GATC motifs	No. of GATC motifs/1,000 bp ^b
<i>pyrD</i>	Pyrimidine biosynthesis	12.6	1,011	13	12.9
<i>dmsA</i>	Dimethyl sulfoxide reductase, anaerobic respiration	7.2	2,445	20	8.2
<i>rlmL</i>	rRNA methylation, methyltransferase	7.9	2,109	21	10.0
<i>uup</i>	Possible role in replication fork progression	6.0	1,908	14	7.3
<i>mukF</i>	Chromosome segregation	5.6	1,323	12	9.1
<i>smtA</i>	S-Adenosylmethionine-dependent methyltransferase	3.9	786	7	8.9
<i>ybiW</i>	Predicted pyruvate formate lyase	4.2	2,433	18	7.4
<i>etk</i>	Protein-tyrosine kinase	3.6	2,181	15	6.9
<i>potI</i>	Putrescine transporter subunit	3.2	846	10	11.8
<i>potH</i>	Putrescine transporter subunit	2.7	954	12	12.6
<i>ygiQ</i>	Unknown, located in operon with <i>ftsP</i>	2.7	2,220	21	9.5
<i>nfrA</i>	Bacteriophage N4 receptor	2.6	2,973	14	4.7

^a Taken from time point B.

^b *Escherichia coli* K-12 has an average of 4.1 GATC motifs per 1,000 bp.

comparison was then repeated for a culture sampled shortly after synchronized initiation of replication (time point C). Figure 6 shows a detailed view of the SeqA and RNA polymerase binding data across the region encompassing both *oriC* and the *rrnC* rRNA operon at time point C. The inverse correlation between the binding of SeqA and RNA polymerase is most apparent in the *rrnC*

operon, which has a lower GATC content than the surrounding DNA.

Evolution of the SeqA regulon. Since SeqA binding in *E. coli* K-12 is linked to the local density of GATC motifs, it might be possible to identify putative SeqA binding sites in other bacteria on the basis of their GATC content. Thus, we identified 123 bac-

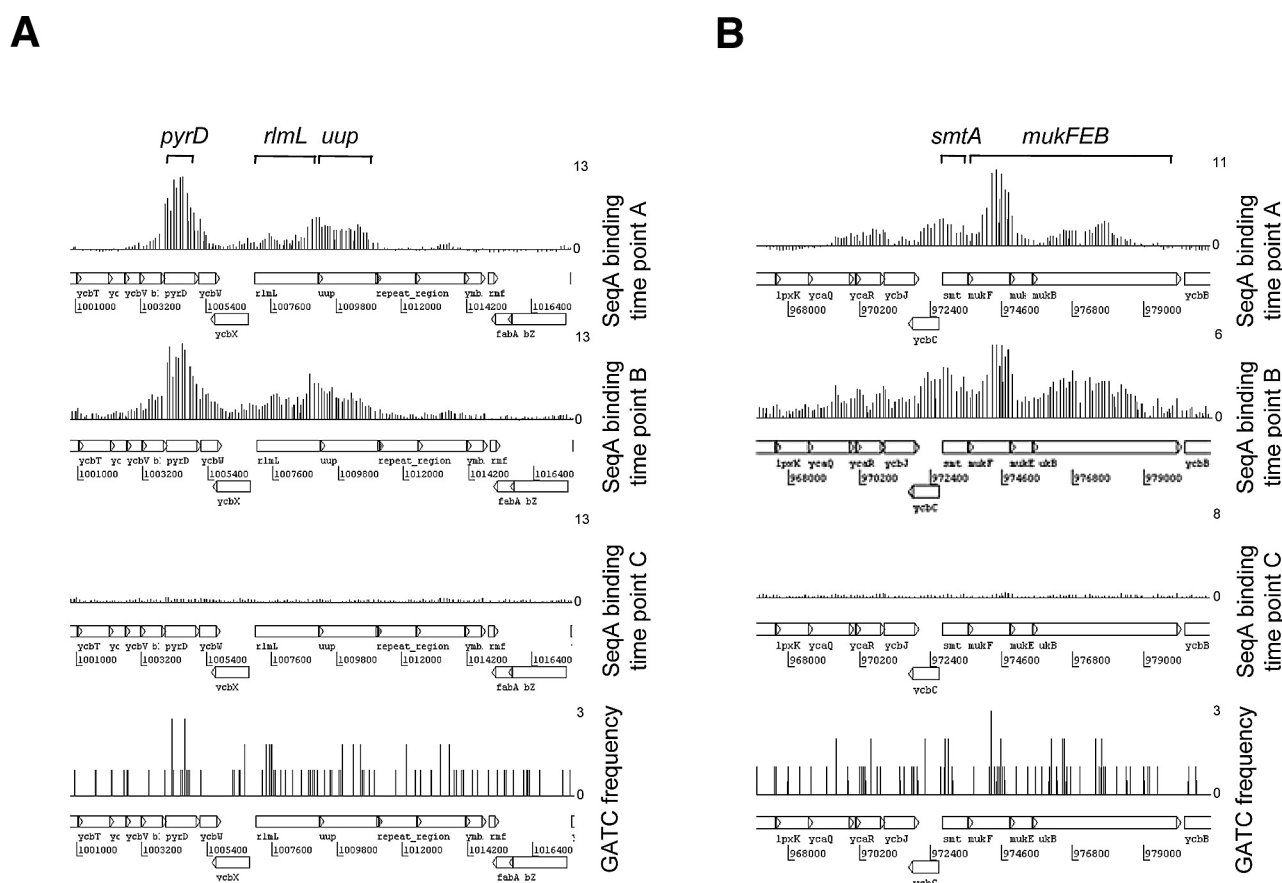


FIG 5 Stable SeqA binding targets. The figure shows ChIP-chip data for SeqA binding close to the *pyrD* (A) and *mukF* (B) genes *in vivo*. Data presented were generated from unsynchronized cultures of *E. coli* (time point A), cultures where chromosome replication had been blocked for 1 h (time point B), and cultures where chromosome replication had been reinitiated in synchronicity for a period of 6 min (time point C). The ChIP-chip data sets have been aligned with a graph showing the locations and frequencies at which GATC sites occur in the underlying DNA sequence.

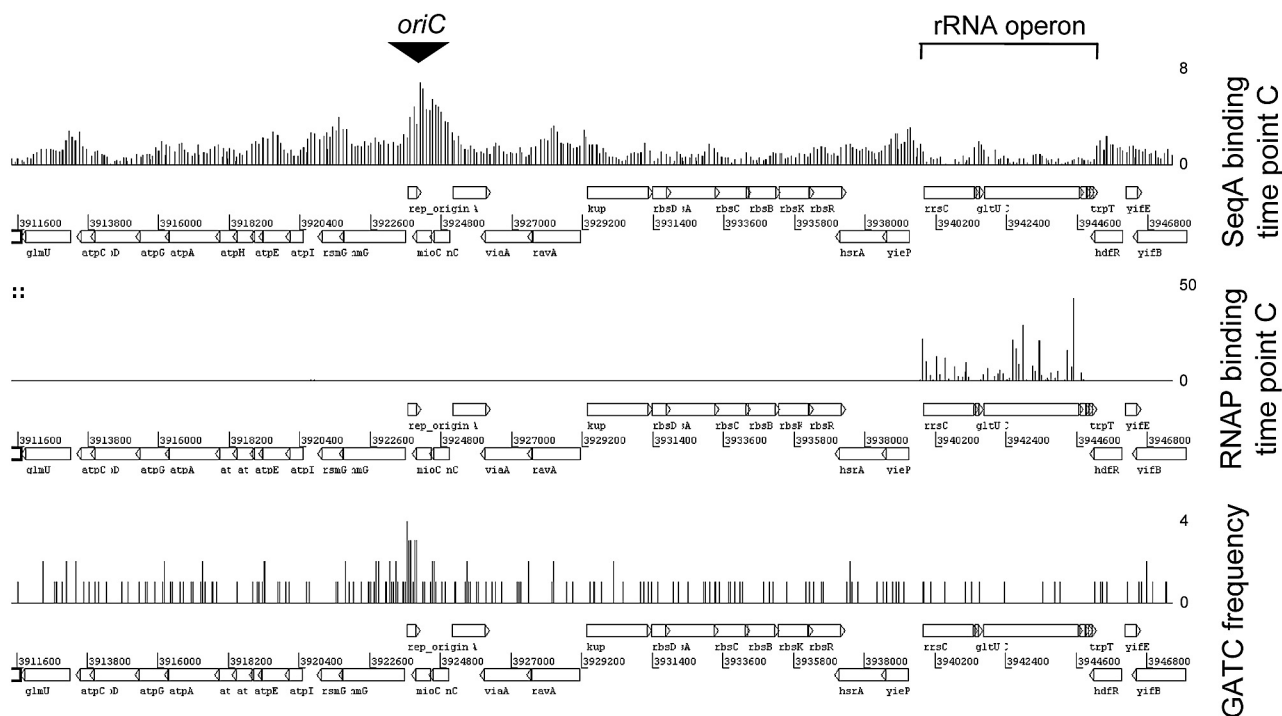


FIG 6 SeqA binding is reduced in rRNA operons. The figure shows ChIP-chip data for SeqA and RNA polymerase binding close to the replication origin and the *rrnC* rRNA operon. The data were generated from synchronized cultures of *E. coli* where chromosome replication had been reinitiated in synchronicity for a period of 6 min. The ChIP-chip data sets have been aligned with a graph showing the locations of and frequencies at which GATC sites occur in the underlying DNA sequence.

terial genomes with a SeqA homologue. We then searched each genome for homologues of the genes listed in Table 1. If a candidate homologue was identified, the sequence was extracted and the density of GATC motifs was calculated for that gene. For each gene, we then compared the GATC density with the average GATC density across the whole of the corresponding genome, and the results are shown in Fig. 7 as a heat map (a higher-resolution version is shown in Fig. S3 in the supplemental material). The figure shows that most of the candidate genes have an increased density of GATC motifs in most genomes. Closer inspection shows that the genomes with SeqA homologues fall into five major evolutionary groups and that the frequency of occurrence of GATC sites in the selected genes is different for each group. The best conservation of above-average GATC frequency is seen in group 1A, which contains *E. coli* K-12 and closely related organisms. Conversely, there is hardly any retention of higher-than-average GATC frequency in group 2B, containing more distantly related genomes. Note that in many cases, this is because the target gene is simply not present (plotted as zero in Fig. 7). For example, *Shewanella frigidimarina* lacks *mukF*, *ybiW*, and *nfrA*, while *Haemophilus somnus* lacks *pyrD*, *smtA*, *ybiW*, *etk*, *potI*, *potH*, *nfrA*, and *ygiQ*.

DISCUSSION

Previous attempts to define regions of the chromosome targeted by SeqA have relied on biochemistry, bioinformatics, and transcriptome analysis (31). Here, we have exploited ChIP-chip assays, which directly measure chromosome-wide DNA binding *in vivo*, to show that SeqA binding is dynamic and responsive to changes in the cell cycle and that it aligns with numerous genes

that play key roles in cell replication. Our data are consistent with previous studies of cell cycle-dependent gene expression (13, 32–37). Thus, we observed SeqA binding to the *dnaA*, *mukB*, *nrdA*, *seqA*, *mioC*, and *gidA* genes, which are transiently repressed as they are replicated, but no binding at the *minE*, *tus*, *ftsY*, *YEK*, and *rpoH* loci, which are not subject to cell cycle-dependent regulation (37, 38). We note that many of the SeqA binding signals observed here stretch across thousands of base pairs, and possibly this is due to the formation of SeqA-DNA filaments that have been observed *in vitro* or looped domains (8, 39, 40).

SeqA binding correlates well with regions of high GATC content, and our analysis showed that a spacing of close to 10 or 20 nucleotides between GATC motifs was most favorable for SeqA binding. Additionally, a GATC motif spacing of ~50 nucleotides or more resulted in only low levels of SeqA binding (Fig. 4). This is consistent with previous *in vitro* studies (8). Interestingly, the highly expressed rRNA operons have evolved to have a particularly low occurrence of GATC sequences; the average number of these motifs per 1,000 bp for all seven *rrn* operons is 1.9, compared to a genome average of 4.1. Thus, we observed particularly low levels of SeqA binding to the rRNA genes (Fig. 6). We suggest that this represents a strategy used by the cell to minimize the effects of DNA replication on rRNA transcription.

The SeqA binding profile generated from unsynchronized cultures (Fig. 2A) gives an averaged view of SeqA binding at all points in the cell cycle. Interestingly, there is a lack of SeqA binding across an ~1.3-Mbp segment that corresponds to the chromosomal “Ter” macrodomain (41). This region is depleted in GATC motifs, consistent with the lack of SeqA binding signal observed. We spec-

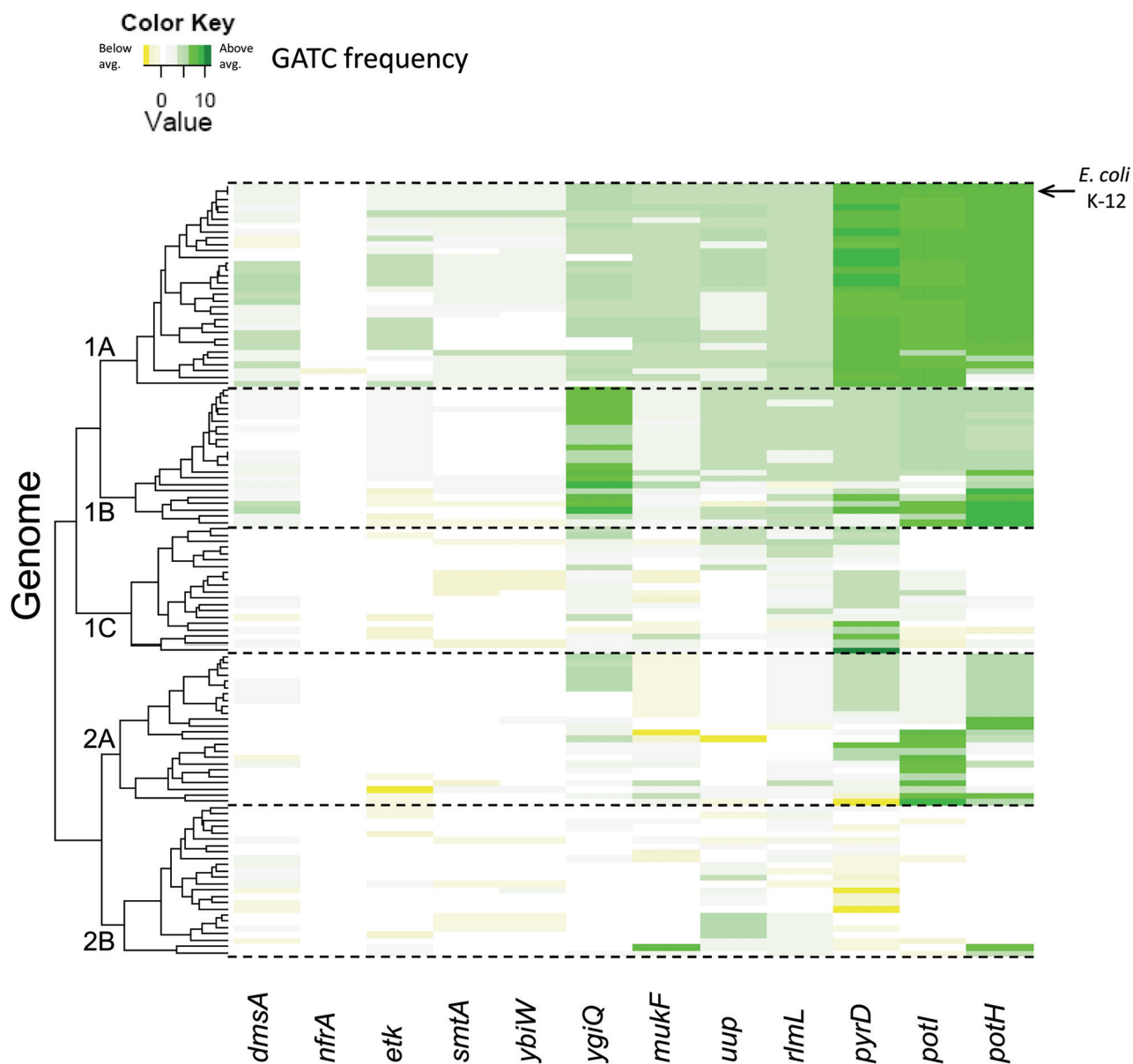


FIG 7 Conservation of GATC motifs in SeqA binding targets. The figure shows a heat map describing the GATC motif contents of 123 bacterial genomes containing a *seqA* homologue (rows) and a group of genes bound by SeqA in our ChIP-chip analysis (columns). Genes that have a higher frequency of GATC motifs than the genome background are green, and genes with an average or less-than-average GATC motif content are yellow. The genomes are clustered into evolutionary groups. Group 1A contains *Enterobacteriaceae*, such as *E. coli* and *Shigella*, and group 1B also contains *Enterobacteriaceae*, including *Salmonella* and *Klebsiella*. Group 2B contains other gammaproteobacteria, such as *Pasteurella multocida*. A high-resolution version of this figure, complete with genome accession numbers, is available in the supplemental material (Fig. S3).

ulate that the asymmetry in the chromosome-wide DNA binding profile of SeqA may be important for defining the orientation of nucleoids within the cell. Alternatively, the binding of SeqA could be reduced in this region to allow convergent replication forks to fuse correctly and complete genome duplication. Note that SeqA can be forced to bind in the *ter* region when new replication events are blocked (Fig. 2B). This is likely because high-affinity SeqA binding sites elsewhere in the genome have become fully methylated, so SeqA binds to the few remaining hemi-methylated GATC motifs that are in the *ter* region. Thus, upon the induction of a fresh round of replication, hemi-methylated GATC motifs arise

elsewhere in the chromosome and SeqA rapidly dissociates from the *ter* region and rebinds *oriC* (Fig. 2C). Thus, progression of the replication fork triggers waves of SeqA relocation from hundreds of targets synchronized with the cell cycle.

SeqA binding is known to persist at some loci after passage of the replication fork (13). We identified several such sites, and one of these, the *pyrD* gene, overlaps a region previously found to remain associated with SeqA for some time after its replication (42). We suggest that SeqA either prevents full methylation of these targets by Dam or is able to bind these targets even when they are fully methylated. Note that we did not observe large changes in

the expression of genes such as *pyrD* under conditions where SeqA was or was not bound (data not shown). We speculate that SeqA plays subtle roles at these targets that will be revealed only by focused studies. For example, SeqA-dependent effects may rely on the binding of other factors, such as transcriptional activators and repressors, that occurs only under specific conditions. Since we observed an overall negative correlation between the binding of RNA polymerase and SeqA, we suggest that SeqA binding most frequently hinders transcription (Fig. 6; see also Fig. S4 in the supplemental material).

The evolution of SeqA binding targets in *E. coli* and closely related pathogens is similar, but some more distantly related bacteria have a different set of SeqA targets (Fig. 7). This may be representative of different lifestyles, or SeqA may play a different role in those organisms. We note that recent studies of transcriptional regulatory proteins also conclude that, despite being conserved between organisms, regulators often control the transcription of different sets of genes (43, 44). In summary, SeqA binds to hundreds of targets distal to the replication origin, and by studying each of these targets in detail, previously undefined roles for SeqA in cell cycle regulation will be uncovered.

MATERIALS AND METHODS

***E. coli* strains and growth.** Strain CMT940 of *E. coli* K-12 was used for all experiments. CMT940 is a thermosensitive derivative of CM735 (45) into which the *dnaC2* allele (27) was introduced by P1 transduction from strain PC2 (28). For all experiments, 50-ml cultures of *E. coli* CMT940 were grown in LB medium in a shaking water bath set at either 30°C (to permit chromosome replication) or 42°C (to block chromosome replication).

Thymidine incorporation assays and flow cytometry. [³H]thymidine incorporation was used to track rates of DNA synthesis in cultures. Pulse labeling of cells with [³H]thymidine and subsequent measurement of trichloroacetic acid (TCA)-insoluble radioactivity in culture samples were done as described by Onogi et al. (46). DNA content per cell was measured by flow cytometry using a Bryte HS (Bio-Rad) cytometer.

ChIP and DNA microarray analysis. ChIP assays were used to measure chromosome-wide DNA binding profiles of SeqA or RNA polymerase in synchronized and unsynchronized cultures of *E. coli* CMT940 using the protocols of Grainger and Busby (23). Assays were done in duplicate, and values presented here are averages of the results of those experiments. Briefly, cultures of *E. coli* CMT940 were treated with 1% formaldehyde and broken open by sonication, which also fragments cross-linked nucleoprotein. Cross-linked SeqA-DNA or RNA polymerase-DNA complexes were immunoprecipitated from cleared lysates by using rabbit polyclonal anti-SeqA antisera (kindly given by Felipe Molina and Kirsten Skarstad) or anti-RNA polymerase sera (Neoclone, Madison, WI). Parallel samples were isolated in mock precipitations with no antibody. Cross-links were then reversed, and after purification, DNA samples isolated with and without antibody were labeled with Cy5 and Cy3, respectively. To identify segments of DNA specifically associated with SeqA, the two labeled samples were combined and hybridized to a 43,450-feature DNA microarray (Oxford Gene Technology, Oxford, United Kingdom). For each probe, the Cy5/Cy3 ratio was measured, and this was plotted against the corresponding position on the *E. coli* chromosome, creating a profile of SeqA binding. Data presented here are the averages of results from replicate experiments and have been normalized so that the average Cy5/Cy3 ratio is 1. ChIP-chip data are presented using DNAPlotter (47) and the Artemis genome browser (48). The full data sets can be accessed in the supplementary tables, where they are in a format that can be viewed using DNAPlotter/Artemis, both of which are freely available at <http://www.sanger.ac.uk/Software>. Table S1 in the supplemental material is an annotation of the *E. coli* genome, and Tables S2 to S4 are averaged data sets from replicate SeqA ChIP-chip experiments. Users should first launch

either DNAPlotter or Artemis. Table S1 in the supplemental material should then be opened before data in Table S2, S3, or S4 are added as a graph. Raw array data are in Table S5 in the supplemental material.

DNA sequence analysis. To calculate the frequency of GATC motifs in *E. coli*, the genome sequence was divided into 60-bp windows. The number of GATC sequences in each window was plotted against the appropriate position on the genome and transferred to an Artemis-compatible file that is shown in Table S6 in the supplemental material.

To calculate the frequencies at which GATC motifs occur in potential SeqA binding targets in other organisms, we first identified all publically available complete bacterial genomes or whole-genome shotgun (WGS) sequences that contained a homologue of SeqA using BLASTp with an E value of $<10^{-7}$. For each of the 221 identified genomes, the average GATC frequency per 1,000 bp was calculated as the total number of GATC motifs divided by genome size (kilobase pairs). Homologues of the SeqA targets *pyrD*, *dmsA*, *rlmL*, *uup*, *murK*, *smtA*, *ybiW*, *etk*, *potI*, *potH*, *ygiQ*, and *nfrA* were identified in each genome using BLASTp, with an E value of $<10^{-5}$. If multiple genes were detected in each genome, only the highest BLAST hit was taken. If a homologous gene was detected, the number of GATC motifs per 1,000 bp was calculated for that gene. Homologues of all 12 potential SeqA binding loci were not found in every genome, specifically in incomplete WGS sequences; therefore, 98 WGS sequences under 500 kbp in length were excluded from further analysis. The difference between the average GATC frequency of each genome and the GATC frequency of specific genes was calculated and plotted in a heat map using the statistical package R (49). If a potential SeqA target gene was absent from a genome, then differences in GATC frequency could not be determined and therefore were plotted as zero.

ACKNOWLEDGMENTS

This work was funded by a Wellcome Trust program grant to S.J.W.B. and a Wellcome Trust Research Career Development Fellowship awarded to D.C.G.M.A.S.-R. is a Marie Curie Early Stage Researcher on the DNAREC program.

We thank Peter McGlynn and Josep Casadesus for critically reading the manuscript and Alan Grossman and Alfonso Jiménez-Sánchez for encouragement and helpful discussions. We are grateful to Felipe Molina and Kirsten Skarstad for the gift of anti-SeqA antibodies, Elena Guzmán for her help with flow cytometry, and María Rosario Sepulveda for advice and support.

SUPPLEMENTAL MATERIAL

Supplemental material for this article may be found at <http://mbio.asm.org/content/1/1/e00012-10.full#SUPPLEMENTAL>.

Table S1, TXT file, 13.2MB.
 Table S2, TXT file, 14.3MB.
 Table S3, TXT file, 14.3MB.
 Table S4, TXT file, 14.3MB.
 Table S5, XLS file, 39.3MB.
 Table S6, TXT file, 13.9MB.
 Table S7, DOC file, 15.8MB.
 Figure S1, PDF file, 12KB.
 Figure S2, PDF file, 46KB.
 Figure S3, PDF file, 161KB.
 Figure S4, PDF file, 53KB.

REFERENCES

- Higgins, N. P. 2007. Mutational bias suggests that replication termination occurs near the dif site, not at Ter sites: what's the dif? *Mol. Microbiol.* 64:1–4.
- Bramhill, D., and A. Kornberg. 1998. A model for initiation at origins of DNA replication. *Cell* 54:915–918.
- Speck, C., and W. Messer. 2000. Mechanism of origin unwinding: sequential binding of DnaA to double- and single-stranded DNA. *EMBO J.* 20:1469–1476.
- Messer, W. 2002. The bacterial replication initiator DnaA. DnaA and

- oriC*, the bacterial mode to initiate DNA replication. FEMS Microbiol. Rev. 26:355–374.
5. Kornberg, A., and T. A. Baker. 1992. DNA replication. W. H. Freeman, New York, NY.
 6. Boye, E., A. Løbner-Olesen, and K. Skarstad. 2000. Limiting DNA replication to once and only once. EMBO Rep. 1:479–483.
 7. Zyskind, J. W., and D. W. Smith. 1986. The bacterial origin of replication, *oriC*. Cell 46:489–490.
 8. Brendler, T., J. Sawitzke, K. Sergueev, and S. Austin. 2000. A case for sliding SeqA tracts at anchored replication forks during *Escherichia coli* chromosome replication and segregation. EMBO J. 19:6249–6258.
 9. Han, J. S., S. Kang, S. H. Kim, M. J. Ko, and D. S. Hwang. 2004. Binding of SeqA protein to hemi-methylated GATC sequences enhances their interaction and aggregation properties. J. Biol. Chem. 279:30236–30243.
 10. Ogden, G. B., M. J. Pratt, and M. Schaechter. 1988. The replicative origin of the *E. coli* chromosome binds to cell membranes only when hemi-methylated. Cell 54:127–135.
 11. Taghbalout, A., A. Landoulsi, R. Kern, M. Yamazoe, S. Hiraga, B. Holland, M. Kohiyama, and A. Malki. 2000. Competition between the replication initiator DnaA and the sequestration factor SeqA for binding to the hemimethylated chromosomal origin of *E. coli* in vitro. Genes Cells 5:873–884.
 12. Nievera, C., J. J. Torgue, J. E. Grimwade, and A. C. Leonard. 2006. SeqA blocking of DnaA-*oriC* interactions ensures staged assembly of the *E. coli* pre-RC. Mol. Cell 24:581–592.
 13. Campbell, J. L., and N. Kleckner. 1990. *E. coli oriC* and the *dnaA* gene promoter are sequestered from *dam* methyltransferase following the passage of the chromosomal replication fork. Cell 62:967–979.
 14. Bogan, J. A., and C. E. Helmstetter. 1997. DNA sequestration and transcription in the *oriC* region of *Escherichia coli*. Mol. Microbiol. 26: 889–896.
 15. Jakomin, M., D. Chessa, A. J. Bäuml, and J. Casadesús. 2008. Regulation of the *Salmonella enterica* *std* fimbrial operon by DNA adenine methylation, SeqA, and HdfR. J. Bacteriol. 190:7406–7413.
 16. Słomińska, M., G. Konopa, J. Ostrowska, B. Kedzierska, G. Wegrzyn, and A. Wegrzyn. 2003. SeqA-mediated stimulation of a promoter activity by facilitating functions of a transcription activator. Mol. Microbiol. 47: 1669–1679.
 17. Slater, S., S. Wold, M. Lu, E. Boye, K. Skarstad, and N. Kleckner. 1995. *E. coli* SeqA protein binds *oriC* in two different methyl-modulated reactions appropriate to its roles in DNA replication initiation and origin sequestration. Cell 82:927–936.
 18. Brendler, T., A. Abeles, and S. Austin. 1995. A protein that binds to the P1 origin core and the *oriC* 13mer region in a methylation-specific fashion is the product of the host *seqA* gene. EMBO J. 14:4083–4089.
 19. Brendler, T., and S. Austin. 1999. Binding of SeqA protein to DNA requires interaction between two or more complexes bound to separate hemimethylated GATC sequences. EMBO J. 18:2304–2310.
 20. Kang, S., H. Lee, J. S. Han, and D. S. Hwang. 1999. Interaction of SeqA and Dam methylase on the hemimethylated origin of *Escherichia coli* chromosomal DNA replication. J. Biol. Chem. 274:11463–11468.
 21. Løbner-Olesen, A., M. G. Marinus, and F. G. Hansen. 2003. Role of SeqA and Dam in *Escherichia coli* gene expression: a global/microarray analysis. Proc. Natl. Acad. Sci. U. S. A. 100:4672–4677.
 22. Cho, B. K., E. M. Knight, and B. Ø. Palsson. 2008. Genomewide identification of protein binding locations using chromatin immunoprecipitation coupled with microarray. Methods Mol. Biol. 439:131–145.
 23. Grainger, D. C., and S. J. Busby. 2008. Global regulators of transcription in *Escherichia coli*: mechanisms of action and methods for study. Adv. Appl. Microbiol. 65:93–113.
 24. Wade, J. T., K. Struhl, S. J. Busby, and D. C. Grainger. 2007. Genomic analysis of protein-DNA interactions in bacteria: insights into transcription and chromosome organization. Mol. Microbiol. 65:21–26.
 25. Ishikawa, S., Y. Ogura, M. Yoshimura, H. Okumura, E. Cho, Y. Kawai, K. Kurokawa, T. Oshima, and N. Ogasawara. 2007. Distribution of stable DnaA-binding sites on the *Bacillus subtilis* genome detected using a modified chip-chip method. DNA Res. 14:155–168.
 26. Wu, L. J., S. Ishikawa, Y. Kawai, T. Oshima, N. Ogasawara, and J. Errington. 2009. Noc protein binds to specific DNA sequences to coordinate cell division with chromosome segregation. EMBO J. 28:1940–1952.
 27. Carl, P. L. 1970. *Escherichia coli* mutants with temperature sensitive synthesis of DNA. Mol. Gen. Genet. 196:387–396.
 28. Withers, H. L., and R. Bernander. 1998. Characterization of *dnaC2* and *dnaC28* mutants by flow cytometry. J. Bacteriol. 180:1624–1631.
 29. Bach, T., M. A. Krekling, and K. Skarstad. 2003. Excess SeqA prolongs sequestration of *oriC* and delays nucleoid segregation and cell division. EMBO J. 22:315–323.
 30. Grainger, D. C., D. Hurd, M. D. Goldberg, and S. J. Busby. 2006. Association of nucleoid proteins with coding and non-coding segments of the *Escherichia coli* genome. Nucleic Acids Res. 34:4642–4652.
 31. Waldminghaus, T., and K. Skarstad. 2009. The *Escherichia coli* SeqA protein. Plasmid 61:141–150.
 32. Sun, L., and J. A. Fuchs. 1992. *Escherichia coli* ribonucleotide reductase expression is cell cycle regulated. Mol. Biol. Cell 3:1095–1105.
 33. Theisen, P. W., J. E. Grimwade, A. C. Leonard, J. A. Bogan, and C. E. Helmstetter. 1993. Correlation of gene transcription with the time of initiation of chromosome replication in *Escherichia coli*. Mol. Microbiol. 10:575–584.
 34. Sun, L., B. A. Jacobson, B. S. Dien, F. Srien, and J. A. Fuchs. 1994. Cell cycle regulation of the *Escherichia coli nrd* operon: requirement for a *cis*-acting upstream AT-rich sequence. J. Bacteriol. 176:2415–2426.
 35. Ogawa, T., and T. Okazaki. 1994. Cell cycle-dependent transcription from the *gid* and *mioC* promoters of *Escherichia coli*. J. Bacteriol. 176: 1609–1615.
 36. Zhou, P., and C. E. Helmstetter. 1994. Relationship between *ftsZ* gene expression and chromosome replication in *Escherichia coli*. J. Bacteriol. 176:6100–6106.
 37. Zhou, P., J. A. Bogan, K. Welch, S. R. Pickett, H. J. Wang, A. Zaritsky, and C. E. Helmstetter. 1997. Gene transcription and chromosome replication in *Escherichia coli*. J. Bacteriol. 179:163–169.
 38. Gómez-Eichelmann, M. C., and C. E. Helmstetter. 1999. Transcription level of operon *ftsYEX* and activity of promoter P1 of *rpoH* during the cell cycle in *Escherichia coli*. J. Basic Microbiol. 39:237–242.
 39. Guarné, A., T. Brendler, Q. Zhao, R. Ghirlando, S. Austin, and W. Yang. 2005. Crystal structure of a SeqA-N filament: implications for DNA replication and chromosome organization. EMBO J. 24:1502–1511.
 40. Chung, Y. S., T. Brendler, S. Austin, and A. Guarné. 2009. Structural insights into the cooperative binding of SeqA to a tandem GATC repeat. Nucleic Acids Res. 37:3143–3152.
 41. Mercier, R., M. A. Petit, S. Schbath, S. Robin, M. El Karoui, F. Boccard, and O. Espéli. 2008. The MatP/matS site-specific system organizes the terminus region of the *E. coli* chromosome into a macrodomain. Cell 135:475–485.
 42. Yamazoe, M., S. Adachi, S. Kanaya, K. Ohsumi, and S. Hiraga. 2005. Sequential binding of SeqA protein to nascent DNA segments at replication forks in synchronized cultures of *Escherichia coli*. Mol. Microbiol. 55:289–298.
 43. Perez, J. C., and E. A. Groisman. 2009. Evolution of transcriptional regulatory circuits in bacteria. Cell 138:233–244.
 44. Perez, J. C., D. Shin, I. Zwir, T. Latifi, T. J. Hadley, and E. A. Groisman. 2009. Evolution of a bacterial regulon controlling virulence and Mg²⁺ homeostasis. PLoS Genet. 5:e1000428.
 45. Hansen, E. B., T. Atlung, F. G. Hansen, O. Skovgaard, and K. von Meyenburg. 1984. Fine structure genetic map and complementation analysis of mutations in the *dnaA* gene of *Escherichia coli*. Mol. Gen. Genet. 196:387–396.
 46. Onogi, T., K. Ohsumi, T. Katayama, and S. Hitaga. 2002. Replication-dependent recruitment of the β -subunit of DNA polymerase III from cytosolic spaces to replication forks in *Escherichia coli*. J. Bacteriol. 184: 867–870.
 47. Carver, T., N. Thomson, A. Bleasby, M. Berriman, and J. Parkhill. 2009. DNAPlotter: circular and linear interactive genome visualization. Bioinformatics 25:119–120.
 48. Rutherford, K., J. Parkhill, J. Crook, T. Horsnell, P. Rice, M. A. Rajandream, and B. Barrell. 2000. Artemis: sequence visualization and annotation. Bioinformatics 16:944–945.
 49. R Development Core Team. 2008. R: a language and environment for statistical computing. R Foundation for Statistical Computing, Vienna, Austria. <http://www.R-project.org>.